PHYSICAL REVIEW B VOLUME 2, NUMBER 2 15 JULY 1970

Dynamical Properties of Quasiparticle Excitations in Metallic Copper

Martin J. G. Lee

The James Franck Institute and Department of Physics, The University of Chicago, Chicago, Illinois 60637
(Received 8 January 1970)

The results of experimental studies of the cyclotron masses associated with various orbits on the Fermi surface of copper are analyzed in terms of an interpolation scheme based on surfaces of constant energy that are constructed by the method of phase-shift analysis. Our results confirm that it is possible to construct surfaces of constant energy that are entirely consistent with experimental Fermi-surface and cyclotron-mass data. The variation of the quasiparticle velocity over the Fermi surface is determined from the experimental cyclotron masses. The anisotropy of the Fermi velocity is in excellent over-all agreement with the results of a similar calculation by Halse, and with recent experimental measurements by Doezema, Koch, and Strom. A comparison between the quasiparticle velocities and the velocities computed from a one-electron potential that has been constructed to fit optical and Fermi-surface data demonstrates that in copper the renormalization of the one-electron energy bands by the electron-phonon interaction varies significantly over the Fermi surface. We find that, for electronic states on the belly, the anisotropy of the renormalization factor is in good qualitative agreement with the predictions of a simple deformation-potential calculation, but that for states within a few degrees of the necks the deformation-potential approximation fails. Encouraged by the partial success of the deformation-potential calculation for virtual electron-phonon processes, we apply similar techniques to discuss the real processes that at low temperatures T contribute a $(1/T^3)$-dependent term to the relaxation time for quasiparticle excitations. We propose a model to describe the variation of the electron-phonon relaxation time over the belly, but conclude that a first-principles calculation may be needed to investigate the relaxation time on the necks. At present there exist insufficient experimental data to allow a convincing test of the accuracy of the model, but it seems likely that our empirical deformation potential will be of value in the analysis of such data when they become available.

INTRODUCTION

The shape of the Fermi surface of copper is known in greater detail than is that of any other metal. Among recent experimental investigations are those of Jan and Templeton,[1] and of O'Sullivan and Schirber,[2] who have measured the absolute de Haas–van Alphen frequencies, and the pressure derivatives of frequency, for certain orbits on the Fermi surface of copper. Their work is complemented by that of Joseph, Thorsen, Gertner, and Valby,[3] and of Halse,[4] who have measured the angular variations of the de Haas–van Alphen frequencies in the ⟨100⟩ and ⟨110⟩ symmetry zones. The experimental de Haas–van Alphen frequencies F may be related to the corresponding extremal cross-sectional areas A of the Fermi surface by the equation

$$F = (\hbar A/2\pi e). \tag{1}$$

Several authors have attempted to deduce the radial distortions of the Fermi surface from the experimental area data[4,5]; their results show that the Fermi surface bulges out along the ⟨111⟩ directions to form necks on the surface of the first Brillouin zone. If the lattice potential in copper were negligible the Fermi surface would be spherical, since for a monovalent fcc metal such as copper the free-electron sphere lies entirely within the first Brillouin zone. The relationship between the Fermi-surface distortions found experimentally, and the strength of the electron-ion interaction in copper, has been investigated by the method of phase-shift analysis.[5] It was found that the necks are caused by a strong d resonance in the electron-ion interaction, which is related to the position of copper close to the end of the $3d$ transition series in the Periodic Table. From the phase-shift analysis, it proved possible to construct a nonlocal effective potential for the electron-ion interaction in copper, such that the shape of the computed Fermi surface, and the band gaps corresponding to certain optical transitions, are in satisfactory agreement with experimental data.

The most complete experimental study of cyclotron masses in copper is that of Koch, Stradling, and Kip.[6] Their work was based on the technique of Azbel'-Kaner cyclotron resonance. Cyclotron masses have also been measured by Smith,[7] in the course of cyclotron resonance studies, and by Joseph, Thorsen, Gertner, and Valby[3] by the de Haas–van Alphen technique. While the masses

obtained from de Haas–van Alphen-effect data are usually less accurate than those from cyclotron resonance studies, the frequency of the de Haas–van Alphen oscillations helps one to relate the observed masses to the corresponding orbits on the Fermi surface. Furthermore, the phase of the de Haas–van Alphen oscillations is relatively high, and the experimental masses are therefore less subject to error through mass spread. The overall agreement between masses obtained by the two techniques suggests that earlier difficulties of measurement[8] and intepretation[9] of the cyclotron resonance data have now been largely overcome.

Doezema, Koch, and Strom[10] have measured the quasiparticle velocities at a few points on the Fermi surface of copper, in the course of an investigation of electron surface-state resonances. The experimental data yield extremal values of the quantity (K/V_F^3), where K is the local radius of curvature of the Fermi surface in the plane normal to the magnetic field, and V_F is the Fermi velocity.[11] Since the radius of curvature is known from experimental Fermi-surface data, it is evidently possible to determine the local value of the Fermi velocity. Unfortunately, direct measurement of the Fermi velocity by this technique is possible only in symmetry directions. Elsewhere, one can do little more than test the consistency of a given model of the anisotropy of (K/V_F^3), since with present experimental techniques the location of the extrema of this function on a belt around the Fermi surface cannot be determined independently.

Halse[4] has determined the anisotropy of the quasiparticle velocity over the Fermi surface of copper in a rather less direct manner. He employed the method described by Roaf[9] to construct an analytic model of surfaces of constant energy in wave-vector space. The electronic energy was expressed as a Fourier series whose coefficients were adjusted to fit the extremal cross-sectional areas of certain orbits on the Fermi surface, as determined from experimental de Haas–van Alphen frequencies. The cyclotron mass of an orbit is defined by $m_H = (\hbar^2/2\pi)(\partial A/\partial E)$; it is proportional to the rate of change of the area of the orbit in wave-vector space with respect to energy. Halse was able to construct a second surface of constant energy, corresponding to an energy slightly greater than the Fermi energy, such that the extremal area of a given orbit on this surface is greater than that on the Fermi surface by an amount proportional to the experimental cyclotron mass. He found that the cyclotron-mass data could be described consistently in this way; this conclusion has been confirmed by recent work of Dresselhaus.[12] The Fermi velocity is defined by $V_F = (1/\hbar)(\partial E/\partial k)$. Hence, the normal distance between the two adjacent surfaces of constant energy is inversely proportional to the local value of the Fermi velocity, and Halse was able to interpret the cyclotron-mass data to yield the anisotropy of the quasiparticle velocity over the Fermi surface.

In the present paper, we apply the method of phase-shift analysis to investigate the dynamical properties of quasiparticle excitations in metallic copper. We begin by outlining the method of phase-shift analysis, and the theory of the renormalization of one-electron properties of metals by the electron-electron and electron-phonon interactions. We then apply the phase-shift method to construct surfaces of constant energy in wave-vector space in order to interpolate the experimental cyclotron-mass data. From the interpolation scheme for the cyclotron masses we determine the anisotropy of the Fermi velocity in copper, and find results in good over-all agreement with those of Halse. A comparison between the quasiparticle velocities deduced in this way and the band velocities computed from the nonlocal one-electron potential discussed above, demonstrates that in copper the renormalization of the one-electron energy bands by the electron-phonon interaction is significantly anisotropic. We find that, except within a few degrees of the necks, the anisotropy of the renormalization factor may be described by a simple deformation potential analysis. We conclude by discussing the implications of this result for the anisotropy of the temperature-dependent component of the relaxation time that is associated with the scattering of quasiparticle excitations by thermally excited phonons.

THEORY

A. Phase-Shift Analysis

A full discussion of the method of phase-shift analysis as it is applied to study Fermi-surface distortions may be found elsewhere.[13] However, it may be helpful to outline the main ideas. The eigenfunctions of energy for an electron propagating in a lattice of scattering centers are solutions of a self-consistent multiple-scattering problem in which an incident wave is scattered by each lattice site with s, p, d, etc., phase shifts, and the scattered wavelets combine to reproduce the initial disturbance. If the lattice potential may be neglected (i.e., if all phase shifts may be set equal to zero), then evidently the solutions of the multiple-scattering problem are plane waves. These solutions correspond to the free-electron model of electrons in metals. Since the system of free electrons is isotropic, the Fermi surface must be spherical.

In real metals, the Fermi surface is distorted by the electron-ion interaction. It is convenient to characterize this interaction by a short-range potential of muffin-tin form, and to describe the scattering of electrons by the lattice by a series of energy-dependent phase shifts. It is not difficult to show that if a nonlocal (energy- and angular-momentum-dependent) potential is assumed, the effects of exchange and correlation, as well as certain relativistic effects, may be folded into the phase shifts. When the electron-ion interaction is taken into account, the self-consistent solutions of the multiple-scattering problem are no longer plane waves, but are complicated functions of Bloch form. The dispersion relation for electrons in a lattice of muffin-tin potentials was first obtained by Slater.[14] The electronic energy levels $E_n(\vec{k})$ associated with a given reduced wave vector $\vec{k}$ are roots of the secular equation

$$\det\{[(\vec{k}+\vec{g})^2 - E]\,\delta_{\vec{g}\vec{g}'} + \Gamma_{\vec{g}\vec{g}'}(\vec{k}, E, \eta_l(E))\} = 0\,, \quad (2)$$

where $\vec{g}, \vec{g}'$ are reciprocal-lattice vectors, and Γ is a function of the reduced phase shifts $\eta_l(E)$ from which all integer multiples of π have been subtracted. The explicit form of the function Γ has been discussed elsewhere.[15]

If one knows the set of reduced phase shifts $\eta_l(E_F)$ appropriate to the Fermi energy, then the shape of the Fermi surface may be computed by plotting the roots of the secular equation (2) as a function of the orientation of the wave vector $\vec{k}$. It follows that the shape of the Fermi surface is fully determined by the set of scattering phase shifts appropriate to the Fermi energy. If the energy-dependent phase shifts $\eta_l(E)$ are known for energies close to the Fermi energy, then not only the shape of the Fermi surface, but also the form of the energy bands close to the Fermi energy, may be computed. Conversely, experimental information concerning the shapes of the Fermi surfaces and the band structures of metals may be interpreted to yield the phase shifts at the Fermi energy and their energy dependences.

Such an analysis has been carried out for copper.[5] The *s*, *p*, *d*, and *f* phase shifts, and the Fermi energy parameter E_F, were adjusted to bring the shape of a surface of constant energy into agreement with experimental Fermi-surface data.[16] The radial distortions of the model surface were in excellent agreement with the radial distortions of the Fermi surface of copper obtained by Halse by an independent technique. Furthermore, the phase shifts deduced from the experimental Fermi-surface data were found to be in fair agreement with those deduced from the semiempirical one-electron potential of Chodorow.[17] Since Chodorow's potential was devised to fit spectroscopic data for the Cu^+ ion, and presumably includes the dominant effects of exchange and correlation, it is perhaps not surprising that it proves to be a good starting point for calculations of the phase shifts. We found that first-principles calculations of the phase shifts tend to be less accurate, presumably because methods of computing exchange and correlation corrections from first principles are little understood.

It would be of interest if we could deduce the form of the effective one-electron potential in copper from the phase shifts associated with the electron-ion interaction. However, exchange and correlation corrections are known to be energy and angular-momentum dependent, so presumably the best one-electron potential would also depend on energy and angular momentum. Furthermore, from the experimental data we may determine the phase shifts at only one energy, the Fermi energy. Evidently, we have not sufficient information to construct a unique effective one-electron potential. However, it is not difficult to construct a nonlocal potential that is entirely consistent with the experimental Fermi-surface data, by adding a nonlocal correction to any potential that is known to give an approximate fit to the data. This procedure may seem somewhat arbitrary, since by starting with different local potentials it is, in principle, possible to generate any number of different nonlocal potentials, each of which gives a perfect fit to the experimental Fermi-surface data. We may choose between these potentials by demanding that the final potential should be consistent not only with experimental Fermi-surface data, but also with the results of optical experiments. Gerhardt[18] has compared the energy gaps computed from various one-electron potentials that have been proposed for metallic copper, with the results of experimental studies of the energies associated with several interband transitions. Of the potentials considered, that of Chodorow gave optical band gaps in the closest agreement with the experimental data. For this reason, we chose to modify the Chodorow potential to fit the Fermi-surface data. To the Chodorow potential, we added an angular-momentum-dependent correction that was taken to be a constant within each muffin-tin sphere, and zero elsewhere. The correction was adjusted to bring the phase shifts deduced from the corrected potential into agreement with those deduced from the experimental data; we found that only a small correction (typically, 0.02 Ry)[19] was necessary to achieve this. The nonlocal Chodorow potential derived in this way implies Fermi-surface distortions and optical energy gaps that are in good agreement with the experimental

data. In the present paper, we shall compute from this potential the form of the energy bands of copper close to the Fermi energy, in order to investigate the renormalization of the one-electron energy bands by the electron-phonon interaction.

B. Renormalization

The effect of a weak slowly varying perturbing potential $\mathfrak{U}(\vec{r})$ on an electron in a metallic lattice may be described in terms of the equivalent Hamiltonian.[20] The effect of the lattice potential is taken into account implicitly; the kinetic-energy operator $E(-i\vec{\nabla})$ in the equivalent Hamiltonian is derived from the form of the one-particle excitation spectrum $E(\vec{k})$. If the perturbing potential is sufficiently slowly varying (an approximation that is usually valid for electrons in metals) the trajectories followed by wave-packet solutions of the equivalent Schrödinger equation are themselves solutions of the classical equations of motion derived from the Hamiltonian function $[E(\vec{k})+\mathfrak{U}(\vec{r})]$. The classical equations of motion lead to an expression for the velocity of an electron of wave vector $\vec{k}$ [21]:

$$V(\vec{k}) = (1/\hbar)\,\nabla_{\vec{k}}\, E(\vec{k}) \quad . \tag{3}$$

In a magnetic field, the Lorentz force causes the wave vector to describe an orbit on a surface of constant energy. The frequency of rotation is usually expressed in terms of the cyclotron mass m_H, which, for an electron whose wave vector lies on the Fermi surface, is given by[22]

$$m_H = \frac{\hbar}{2\pi} \oint_{\text{orb}} \frac{d\vec{k}}{V_\perp(\vec{k})} \tag{4}$$

or

$$m_H = \frac{\hbar^2}{2\pi} \frac{\partial A}{\partial E} \quad , \tag{5}$$

where $V_\perp(\vec{k})$ is the velocity component normal to, and in the plane of, the orbit and A is the extremal cross-sectional area of the Fermi surface in a plane normal to the direction of the magnetic field.

Experimentally, one explores the dynamical properties of quasiparticle excitations of the system of interacting electrons in a metal, rather than the dynamical properties of bare electrons. For this reason it is not surprising that calculations based on (4) and (5), in which the excitation spectrum is taken from a band-structure calculation based on a one-electron potential such as the nonlocal Chodorow potential, fail to yield Fermi velocities and cyclotron masses in agreement with experimental data. In order to calculate the quasiparticle excitation spectrum $\epsilon(\vec{k})$ [23] that is appropriate to velocity and cyclotron-mass calculations, it is necessary to take many-body effects into account by evaluating the one-particle propagator $G(\vec{k}, \epsilon)$ for the interacting system

$$G(\vec{k},\epsilon) = [\epsilon - \epsilon^0(\vec{k}) - \sum_{ee}(\vec{k},\epsilon) - \sum_{ep}(\vec{k},\epsilon)]^{-1} , \tag{6}$$

where $\epsilon^0(\vec{k})$ is the bare-electron energy as computed from a one-electron potential and $\sum(\vec{k},\epsilon)$ is the proper self-energy, whose real part describes processes of emission and absorption of virtual photons and virtual phonons by the bare electron, and whose imaginary part describes the decay of quasiparticle excitations caused by electron-electron and electron-phonon interactions. We have decomposed the proper self-energy into two terms, one of which represents the contribution of the electron-electron interaction, the other, that of the electron-phonon interaction.

There is an important qualitative difference between the contributions of the electron-electron and the electron-phonon interactions to the proper self-energy. The electron-electron interaction is known to contribute to a comparable extent to the self-energies of all electonic states; thus, to a large extent, its influence may be folded into a semiempirical one-electron potential. The Coulomb interaction is expected to influence the overall form of the energy bands, and since the nonlocal Chodorow potential was found to predict band gaps that are consistent with the results of optical measurements of the energies associated with several interband transitions, we believe that we have succeeded in folding the dominant Coulomb effects into this potential. As we remarked above, it is perhaps not surprising that only small corrections are needed to achieve this, since the Chodorow potential was itself derived from spectroscopic data and presumably includes certain effects of exchange and correlation. We therefore redefine $\epsilon^0(\vec{k})$ as the excitation spectrum computed from a one-electron potential into which the effects of exchange and correlation have been folded to the greatest possible extent. In this way, the dominant effects of the electron-electron interaction are transferred from the proper self-energy term $\sum_{ee}(\vec{k},\epsilon)$ to the one-particle excitation spectrum $\epsilon^0(\vec{k})$.[24]

The remaining term $\sum_{ep}(\vec{k},\epsilon)$ in the proper self-energy arises from the electron-phonon interaction. In contrast to the behavior of the Coulomb interaction, the electron-phonon interaction contributes significantly to the self-energies of only those quasiparticles whose energies lie within about $\pm\hbar\omega_{\max}$ of the Fermi energy, where $\omega_{\max}$ is the maximum phonon frequency.[25] The electron-phonon interaction modifies those properties of a metal that depend on the derivative of the quasiparticle excitation spectrum at the Fermi surface,

but it does not affect significantly the form of energy bands that lie substantially above and below the Fermi energy. In particular, Fermi velocities and cyclotron masses are strongly influenced by the electron-phonon interaction, while this interaction has little effect on the shapes of Fermi surfaces or on the energies associated with interband transitions in metals.

We now discuss briefly the renormalization of the one-electron energy bands by the electron-phonon interaction. We consider a quasiparticle whose renormalized energy is $\epsilon(\vec{k})$. The electron-phonon contribution to the self-energy of such an excitation in a normal metal at finite temperature is given by the equation[26]

$$\sum_{ep}(\vec{k},\epsilon)=\sum_{\sigma}\int_0^{\infty}d\epsilon'\int_0^{\omega_{max}}\hbar\,d\omega\,\alpha_\sigma^2(\vec{k},\omega)F_\sigma(\omega)\times\{[N(\omega)+f(-\epsilon')][(\epsilon'+\hbar\omega+\epsilon)^{-1}-(\epsilon'+\hbar\omega-\epsilon)^{-1}]+[N(\omega)+f(\epsilon')][(-\epsilon'+\hbar\omega+\epsilon)^{-1}-(-\epsilon'+\hbar\omega-\epsilon)^{-1}]\}, \tag{7}$$

where $\alpha_\sigma^2(\vec{k},\omega)$ is a measure of the strength of the electron-phonon interaction, $F_\sigma(\omega)$ is the phonon density of states, $N(\omega)$ is the Bose-Einstein distribution function, and $f(\epsilon)$ is the Fermi-Dirac distribution function. Equation (7) is the finite temperature generalization of the gap equations of Éliashberg, where since we are concerned with normal metals we have set the gap parameter equal to zero. If we neglect thermal phonons $[N(\omega)=0)]$ and evaluate the integral over ϵ' in the limit of low excitation energy ($\epsilon\ll\hbar\omega_{max}$) and low temperature ($T\to 0$), we find

$$\sum_{ep}(\vec{k},\epsilon)\approx-\epsilon\lambda(\vec{k},0)\ ,$$

where

$$\lambda(\vec{k},0)=2\sum_{\sigma}\int_0^{\omega_{max}}\alpha_\sigma^2(\vec{k},\omega)F_\sigma(\omega)\frac{d\omega}{\omega}\ . \tag{8}$$

In the limit of large energy of excitation ($\epsilon\gg\hbar\omega_{max}$) and low temperature, we find

$$\sum_{ep}(\vec{k},\epsilon)=-\epsilon\lambda(\vec{k},\infty)\ ,$$

where

$$\lambda(\vec{k},\infty)=0\ . \tag{9}$$

The quasiparticle excitation energies $\epsilon(\vec{k})$ are poles of the propagator

$$G(\vec{k},\epsilon)=[\epsilon-\epsilon^0(\vec{k})-\sum_{ep}(\vec{k},\epsilon)]^{-1}\ .$$

The excitation spectrum is therefore

$$\epsilon(\vec{k})=\epsilon^0(\vec{k})-\epsilon(\vec{k})\lambda(\vec{k},\epsilon)$$

or $$\epsilon(\vec{k})=\epsilon^0(\vec{k})/[1+\lambda(\vec{k},\epsilon)]\ .$$

Thus the spectrum of quasiparticle excitations is renormalized by the electron-phonon interaction, the extent of the renormalization being governed by the dimensionless coupling parameter $\lambda(\vec{k},\epsilon)$. The excitation spectrum for low-energy excitations is therefore

$$\epsilon(\vec{k})\approx\epsilon^0(\vec{k})/[1+\lambda(\vec{k},0)]\ , \tag{10}$$

whereas for excitation energies much larger than the maximum phonon energy we find

$$\epsilon(\vec{k})\approx\epsilon^0(\vec{k})\ .$$

In this limit, the excitation spectrum is unaffected by the electron-phonon interaction.

It is not difficult to show that at low temperatures the Fermi velocity and the cyclotron mass are renormalized by the factor $[1+\lambda(\vec{k},0)]$. If we assume an excitation spectrum of the form (10) and compute the Fermi velocity from Eq. (3), we find

$$V(\vec{k})=V^0(\vec{k})/[1+\lambda(\vec{k},0)]\ , \tag{11}$$

where we have neglected the $\vec{k}$ dependence of $\lambda(\vec{k},0)$. The velocity associated with quasiparticle excitations on the Fermi surface is therefore equal to the band velocity $V^0(\vec{k})$ divided by an anisotropic renormalization factor $[1+\lambda(\vec{k},0)]$. Once the renormalized Fermi velocity is known at all points around an orbit on the Fermi surface, the renormalized cyclotron mass for that orbit may be computed from Eq. (4):

$$m_H=\oint_{orb}\{[1+\lambda(\vec{k},0)]/V_\perp^0(\vec{k})\}\,d\vec{k}\ . \tag{12}$$

In principle, the renormalization factor is given by Eq. (8) only in the limit of zero temperature. However, the work of Grimvall[27] suggests that we are justified in neglecting temperature effects at finite but sufficiently low temperatures.

We conclude that the renormalization of the dynamical properties of electrons on the Fermi surface by the electron-phonon interaction is described by the anisotropic factor $[1+\lambda(\vec{k},0)]$, where $\lambda(\vec{k},0)$ is defined by Eq. (8). The dimensionless factor $\alpha_\sigma^2(\vec{k},\omega)F_\sigma(\omega)$ in Eq. (8) describes the coupling of an electron state $\vec{k}$ to all other states by phonons of frequency ω and polarization σ. It is defined by[28]

$$\alpha_\sigma^2(\vec{k},\omega)F_\sigma(\omega)=\frac{\Omega}{(2\pi)^3}\int\frac{dS_{\vec{k}'}}{\hbar V_{\vec{k}'}}\,|M_\sigma(\vec{k},\vec{k}')|\times\delta(\hbar\omega-\hbar\omega_{\vec{k}-\vec{k}',\sigma})\ , \tag{13}$$

where Ω is the volume of the crystal and $V_{\vec{k}'}$ is the Fermi velocity. The integral $dS_{k'}$ is taken over the Fermi surface, and the matrix elements of the electron-phonon interaction are given by[29]

$$M_\sigma(\vec{k},\vec{k}') = \sum_{\vec{g}} (\hbar/2MN\Omega\omega_{\vec{q},\sigma})^{1/2} \delta_{\vec{g},\vec{k}'-\vec{k}-\vec{q}}\, \mathcal{J}_{\vec{q},\sigma}(\vec{k},\vec{k}') , \quad (14)$$

where $$\mathcal{J}_{\vec{q},\sigma}(\vec{k},\vec{k}') = \int \Psi_{\vec{k}}^{*} (\vec{e}_{\vec{q},\sigma}\cdot\vec{\nabla}v)\Psi_{\vec{k}'}\, d^3r \quad (15)$$

is the matrix element for scattering between states $\vec{k}$ and $\vec{k}'$ by a single ion whose displacement is associated with the phonon mode of wave vector $\vec{q}$ and polarization σ. Substituting (13) into (8), and evaluating the integral over ω, we find

$$\lambda(\vec{k},0) = \frac{2\Omega}{(2\pi)^3} \sum_{\sigma} \int \frac{dS_{\vec{k}'}}{\hbar V_{\vec{k}'}} \frac{|M_\sigma(\vec{k},\vec{k}')|^2}{\hbar\omega_{\vec{k}-\vec{k}',\sigma}} . \quad (16)$$

Thus, the factor that describes the renormalization of the one-electron energy of a given state on the Fermi surface by the electron-phonon interaction may be expressed as an integral involving the matrix elements coupling that state to all other states on the Fermi surface. If the phonon spectrum and the matrix elements of the electron-phonon interaction are known, a first-principles calculation of the renormalization of the one-electron energy bands by the electron-phonon interaction may be carried out. Conversely, we may hope to learn something about the electron-phonon interaction in metals by studying the renormalization of one-electron energies as revealed by experimental studies of the cyclotron mass.

RESULTS

A. Cyclotron Masses

In Table I, we have collected the experimentally determined cyclotron masses associated with 14 different orbits on the Fermi surface of copper. Most of the masses are taken from the work of Koch, Stradling, and Kip,[6] but for the four-cornered rosette orbit normal to ⟨100⟩ we have taken the result of Joseph, Thorsen, Gertner, and Valby,[3] since a preliminary analysis suggested that the value quoted by Koch, Stradling, and Kip may be inconsistent with the rest of their cyclotron-mass data.[30] Along with the experimental masses, we have tabulated the band masses computed from the nonlocal Chodorow potential.[31] The extremal cross-sectional area of each orbit was computed both on the Fermi surface and for energies slightly above and below the Fermi energy, using procedures of numerical integration that have been described elsewhere.[13] The band masses were deduced from Eq. (5); the masses derived from the surfaces of constant energy above and below the Fermi energy were averaged to eliminate any errors due to curvature of the energy bands. The magnitude of the energy increment ($\delta E = \pm 0.000\,046$ Ry) was chosen to give computed masses to an accuracy of about 0.2%; a larger energy increment would give somewhat greater accuracy in calculations of the area differences (δA), but the computed quantity ($\delta A/\delta E$) would then correspond less exactly to the differential quantity ($\partial A/\partial E$). Our calculations show that, for each orbit, the experimental cyclotron mass is significantly greater than the band mass. It is convenient to define an orbital mass-enhancement factor

TABLE I. Experimental measurements and band calculations of the cyclotron masses associated with certain orbits on the Fermi surface of copper. All orbit angles are measured from ⟨100⟩. The masses are expressed in units of the free-electron mass.

Orbit	Experimental mass m_H	Band mass m_H^0	Enhancement $(1+\lambda_0)$
Belly 0° in (110)	(1.370 ± 0.005) [a]	1.238(1.245) [b]	(1.107 ± 0.004)
Belly 8° in (110)	(1.365 ± 0.005) [a]	1.229	(1.111 ± 0.004)
Belly 16° in (110)	(1.355 ± 0.005) [a]	1.223	(1.108 ± 0.004)
Belly 24° in (110)	(1.470 ± 0.020) [a]	1.296	(1.134 ± 0.016)
Belly ⊥ ⟨111⟩	(1.385 ± 0.005) [a]	1.277(1.285) [b]	(1.085 ± 0.004)
Four-rosette ⊥ ⟨100⟩	(1.33 ± 0.06) [c]	1.183	(1.124 ± 0.051)
Dog's bone ⊥ ⟨110⟩	(1.290 ± 0.005) [d]	1.126	(1.146 ± 0.004)
Neck 30° in (110)	(0.925 ± 0.050) [a]	0.827	(1.119 ± 0.061)
Neck 40° in (110)	(0.527 ± 0.020) [a]	0.448	(1.176 ± 0.044)
Neck 50° in (110)	(0.467 ± 0.020) [a]	0.380	(1.229 ± 0.052)
Neck ⊥ ⟨111⟩	(0.460 ± 0.020) [a,c]	0.374(0.370) [b]	(1.230 ± 0.053)
Neck 60° in (110)	(0.468 ± 0.020) [a]	0.383	(1.222 ± 0.052)
Neck 70° in (110)	(0.547 ± 0.020) [a]	0.452	(1.210 ± 0.044)
Neck 80° in (110)	(0.926 ± 0.050) [a]	0.804	(1.152 ± 0.062)

[a] Reference 6.

[b] The band masses were computed from the nonlocal Chodorow potential discussed in the text. For comparison, certain band masses derived from the unmodified Chodorow potential (Ref. 17) are included in parentheses.

[c] Reference 3.

[d] Here we have adopted Halse's interpretation (Ref. 4) of the data of Koch, Stradling, and Kip (Ref. 6).

$$(1+\lambda_0)=(m_H/m_H^0) \quad ,$$

where m_H is the experimental cyclotron mass and m_H^0 is the band mass. Numerical values of the orbital mass-enhancement factor are set out in Table I.

Our immediate aim is to make a weighted least-squares fit to the cyclotron-mass data, in order to interpolate the mass data and to determine the variation of the quasiparticle velocity over the Fermi surface. The problem is entirely one of geometry, and rapid convergence of the calculations depends on one making an appropriate choice of the parametrized description of the surfaces of constant energy. For a metal whose Fermi surface is highly convoluted, one might attempt to make a least-squares fit to the cyclotron-mass data by adjusting the phase shifts in the secular determinant (2), but rapid convergence of the phase shifts in l is not assured, and since the relationship between the band masses and the phase shifts cannot be expressed analytically, the calculations would be rather difficult to carry out.

For a metal whose Fermi surface is nearly spherical, an alternative way of interpolating the experimental cyclotron-mass data might be to expand the renormalization factor $[1+\lambda(\vec{k},0)]$ in a truncated series of cubic harmonics[32]

$$[1+\lambda(\vec{k},0)]=1+\textstyle\sum_i \alpha_i K_i(\theta,\phi) \quad . \tag{17}$$

Then, according to Eq. (12), the mass-enhancement factor associated with a given orbit may be expressed as a line integral of the renormalization factor $[1+\lambda(\vec{k},0)]$ around the orbit

$$(1+\lambda_0)=\oint_{\text{orb}} \frac{[1+\lambda(\vec{k},0)]}{V_\perp^0(\vec{k})}\,d\vec{k} \Big/ \oint_{\text{orb}} \frac{1}{V_\perp^0(\vec{k})}\,d\vec{k} \quad , \tag{18}$$

where $V_\perp^0(\vec{k})$ is the component of the band velocity normal to, and in the plane of, the orbit. The coefficients α_i in the cubic harmonic expansion of the renormalization factor (17) may be adjusted, by standard techniques of linear algebra, to achieve a weighted least-squares fit to the orbital mass-enhancement factor.

Such a procedure was carried out to fit the orbital mass-enhancement factors for copper (Table I). The line integrals in (18) were evaluated numerically, using an integration formula based on straight-line segments:

$$dk=(k_1^2+k_2^2-2k_1k_2\cos\theta)^{1/2} \quad ,$$

where k_1 and k_2 are the radii bounding the sector whose vertex angle is θ. We found that adequate accuracy was achieved by reducing the angular interval in the integration formula to 1 deg of arc. The quality of the least-squares fit to the orbital mass-enhancement factors was estimated by evaluating the expression

$$\chi^2=\textstyle\sum[(m_{Hc}-m_{He})/\sigma_e]^2 \quad , \tag{19}$$

where m_{Hc} is the cyclotron mass computed from the interpolation scheme, m_{He} is the experimental value of the cyclotron mass for the same orbit, σ_e is the standard deviation of the experimental value of the mass, and the sum is taken over all orbits. In general, the smaller the value of χ^2, the better is the fit to the experimental data. From tables of the χ^2 distribution, one may estimate the probability that an apparently good fit to the data may, in fact, be without significance. The χ^2 test indicated that our best fit to the orbital mass-enhancement factors involved five cubic harmonics, but that the probability that this fit is significant is no greater than 90%. Presumably the rapid angular variation of the renormalization factor, particularly in the region of the necks, accounts for the relatively poor convergence when one tries to expand it in cubic harmonics.

This suggested a more accurate way of interpolating the mass data. It seemed likely that if model surfaces of constant energy were constructed to fit exactly the cyclotron-mass data for a few orbits, then the correction factor by which the model masses for the remaining orbits must be multiplied to bring them into agreement with the experimental masses would be a slowly varying function of angle, and hence capable of expansion in a rapidly convergent series of cubic harmonics. The s-, p-, and d-phase shifts were adjusted to construct surfaces of constant energy to fit the cyclotron masses of the belly orbit normal to $\langle 100\rangle$, and of the neck and belly orbits normal to $\langle 111\rangle$.[33] A local correction factor $[1+\Lambda(\vec{k})]$ was defined by analogy with Eq. (11):

$$V(\vec{k})=V^p(\vec{k})/[1+\Lambda(\vec{k})] \quad , \tag{20}$$

where $V(\vec{k})$ is the quasiparticle velocity and $V^p(\vec{k})$ is the Fermi velocity computed from the phase-shift model. An orbital correction factor appropriate to the phase-shift model was also defined,

$$(1+\Lambda_0)=(m_H/m_H^p) \quad ,$$

where m_H is the experimental cyclotron mass, and m_H^p is the cyclotron mass computed from the phase-shift model. According to the results set out in Table II, the factor $(1+\Lambda_0)$ is very close to unity for all orbits. Nevertheless, our results suggest that this factor departs from unity in a systematic way, and that its anisotropy should be taken into account. We may expand $[1+\Lambda(\vec{k})]$ in a series of cubic harmonics

$$[1+\Lambda(\vec{k})]=1+\textstyle\sum_i \beta_i K_i(\theta,\phi) \tag{21}$$

TABLE II. The cyclotron masses for certain orbits on the Fermi surface of copper, as computed from the phase-shift model, are interpolated by making a cubic harmonic fit to the correction factor $(1+\Lambda_0)$. The masses derived from this interpolation scheme are compared with the experimental masses. Angles are measured in degrees from ⟨100⟩. Masses are expressed in units of the free-electron mass. m_H^p is the phase-shift model mass, and m_H is the experimental mass. The correction factor is defined by $(1+\Lambda_0)=(m_H/m_H^p)$.

Orbit	m_H^p	Correction $(1+\Lambda_0)$	Interpolated [a] mass	m_H
Belly 0° in (110)	1.373	0.998	1.372	(1.370 ± 0.005)
Belly 8° in (110)	1.360	1.004	1.362	(1.365 ± 0.005)
Belly 16° in (110)	1.348	1.005	1.357	(1.355 ± 0.005)
Belly 24° in (110)	1.441	1.020	1.454	(1.470 ± 0.020)
Belly ⊥ ⟨111⟩	1.386	1.000	1.386	(1.385 ± 0.005)
Four-rosette ⊥ ⟨100⟩	1.323	1.005	1.311	(1.33 ± 0.06)
Dog's bone ⊥ ⟨110⟩	1.283	1.006	1.290	(1.290 ± 0.005)
Neck 30° in (110)	0.970	0.954	0.965	(0.925 ± 0.050)
Neck 40° in (110)	0.545	0.966	0.542	(0.527 ± 0.020)
Neck 50° in (110)	0.467	1.000	0.467	(0.467 ± 0.020)
Neck ⊥ ⟨111⟩	0.460	1.000	0.460	(0.460 ± 0.020)
Neck 60° in (110)	0.469	0.998	0.468	(0.468 ± 0.020)
Neck 70° in (110)	0.551	0.993	0.549	(0.547 ± 0.020)
Neck 80° in (110)	0.943	0.982	0.938	(0.926 ± 0.050)

[a]The best fit to the data was obtained with a four-cubic harmonic expansion of the correction factor which, expressed in the notation of Ref. 32, is $(1+\Lambda_0)=1.005\,{}_1K_0+0.009\,{}_1K_4+0.000\,{}_1K_6-0.033\,{}_1K_8$.

and express the orbital correction factor as a line integral of the local correction factor

$$(1+\Lambda_0)=\oint_{\text{orb}}\frac{[1+\Lambda(\vec{k})]}{V_1^p(\vec{k})}\,d\vec{k}\Big/\oint_{\text{orb}}\frac{1}{V_1^p(\vec{k})}\,d\vec{k}\,. \quad (22)$$

Again, techniques of linear algegra may be employed to adjust the coefficients β_i to make a weighted least-squares fit to the orbital correction factors. The excellent convergence of this procedure is indicated in Table III. Our best fit to the data was achieved with four cubic harmonics. According to the χ^2 test, the probability that this fit to the data is significant is close to 99.1%. It will be seen from the results in Table II that the masses obtained by correcting the phase-shift model masses with the interpolated factor $(1+\Lambda_0)$ agree well with the experimental data.

One might, of course, compute the cyclotron masses of other orbits on the Fermi surface of copper on this way. In the absence of experimental data against which to check the results, we did not consider it worthwhile to undertake such calculations. However, an experimental determina-

TABLE III. Combined phase-shift and cubic harmonic fits to the experimental cyclotron masses in copper. N is the number of cubic harmonics included in the expansion of the orbital correction factor $(1+\Lambda_0)$. χ^2 is the statistical sum computed from Eq. (19). DF (degrees of freedom) is the excess of the number of data points over the number of adjustable parameters. Prob. is the percentage probability that the fit to the data is significant. The best fit to the data is obtained with four cubic harmonics; increasing the number of cubic harmonics beyond four merely reproduces the noise in the data with increased accuracy.

N	χ^2	DF	Prob.
1	9.39	13	74.2
2	7.17	12	84.4
3	5.92	11	88.0
4	2.49	10	99.1
5	2.46	9	98.0
6	2.33	8	97.0
7	2.32	7	94.1

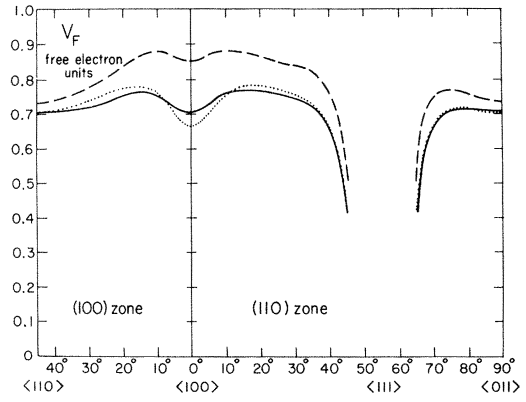

FIG. 1. Angular variations of the Fermi velocity of copper in the (100) and (110) zones. The full curve is a plot of the quasiparticle velocity as deduced from experimental cyclotron-mass data in the course of the present work, while the dotted curve represents the results of calculations by Halse. The broken curve represents the band velocity as computed from the nonlocal Chodorow potential.

TABLE IV. Anisotropy of the Fermi velocity and the renormalization factor on the Fermi surface of copper. The angle from ⟨100⟩ is expressed in deg. θ is the angle between the radius vector from the center of the Brillouin zone to a point on the Fermi surface, and the normal to the Fermi surface at that point. Cosθ is tabulated for reference only.

Angle	cosθ	$V^0(\vec{k}_F)$ [a]	$V(\vec{k}_F)$ [b]	$[1+\lambda(\vec{k},0)]$ [c]
		(100) zone		
⟨100⟩	1.0000	0.853	0.704	1.211 ± 0.014
5°	0.9840	0.868	0.730	1.189
10°	0.9683	0.877	0.753	1.165
15°	0.9709	0.864	0.762	1.134
20°	0.9805	0.835	0.749	1.114
25°	0.9900	0.803	0.734	1.094
30°	0.9958	0.775	0.722	1.072
35°	0.9987	0.753	0.714	1.055
40°	0.9998	0.739	0.708	1.042
⟨110⟩	1.0000	0.733	0.706	1.038 ± 0.012
		(110) zone		
⟨100⟩	1.0000	0.853	0.704	1.211 ± 0.014
5°	0.9831	0.870	0.729	1.193
10°	0.9722	0.879	0.757	1.161
15°	0.9762	0.875	0.768	1.140
20°	0.9907	0.861	0.761	1.131
25°	0.9996	0.849	0.752	1.130
30°	0.9951	0.840	0.742	1.132
35°	0.9707	0.819	0.718	1.141
40°	0.8999	0.754	0.645	1.169
41°	0.8729	0.728	0.618	1.177
42°	0.8314	0.693	0.584	1.188
43°	0.7622	0.650	0.542	1.200
44°	0.5970	0.630	0.520	1.212
neck	•••	0.503	0.413	1.219 ± 0.012
66°	0.6943	0.628	0.527	1.192
67°	0.7890	0.668	0.569	1.175
68°	0.8412	0.702	0.605	1.161
70°	0.8962	0.744	0.655	1.135
75°	0.9579	0.768	0.705	1.088
80°	0.9830	0.755	0.713	1.059
85°	0.9959	0.740	0.710	1.043
⟨110⟩	1.0000	0.733	0.706	1.038 ± 0.012

[a] Band velocity derived from nonlocal potential and expressed in units of 1.5779×10^8 cm/sec (free-electron units).

[b] Quasiparticle velocity derived from best fit to experimental cyclotron-mass anisotropy and expressed in free-electron units.

[c] Renormalization factor defined by $[1+\lambda(\vec{k},0)] = [V^0(\vec{k}_F)/V(\vec{k}_F)]$.

tion of the cyclotron masses of central-belly orbits in planes normal to directions in the (100) zone, and a redetermination of the cyclotron mass associated with the four-cornered rosette orbit, would provide a useful check on our interpolation scheme.

B. Fermi Velocity

Once the best set of coefficients in the cubic harmonic expansion of $[1+\Lambda(\vec{k})]$ has been determined, one may calculate from Eq. (20) the quasiparticle velocity at all points on the Fermi surface. The quasiparticle velocity is plotted in Fig. 1 where, for directions lying in the (100) and (110) zones, it is compared with the band velocity computed from the nonlocal Chodorow potential. The quasiparticle velocity, like the band velocity, is markedly anisotropic, and decreases sharply close to the necks. The anisotropy of the Fermi velocity is set out numerically in Table IV.

In Table V, we compare our estimates of the Fermi velocities in certain directions with velocities obtained by Halse[4] by a Fourier series inversion of experimental cyclotron masses, and with velocities derived by Doezema, Koch, and Strom[10] from an analysis of electron surface-state resonances. The velocities obtained by Halse in the (100) and (110) symmetry zones are also superimposed upon the results of the present calculations displayed in Fig. 1. The two sets of velocities are in excellent over-all agreement with one another, although there is a slight discrepancy close to the ⟨100⟩ direction. The present calculations involve a weighted least-squares fit to 14 cyclotron masses, whereas the earlier calculations of Halse were based on an exact fit to five masses. We believe that the slight discrepancies between our results and those of Halse may reflect the larger number of pieces of experimental data included in the present calculations.

Our results for the Fermi velocities in the ⟨100⟩ direction and on the neck are in good agreement with those of Doezema, Koch, and Strom[10]; our estimate of the anisotropy of the Fermi velocity in the (100) and (110) zones, when combined with experimental information concerning the radius of curvature of the Fermi surface, should provide a

TABLE V. Comparison of estimates of the quasiparticle velocities in copper. The velocities are expressed in units of 1.5779×10^8 cm/sec (free-electron units).

Direction	⟨100⟩	⟨110⟩	Neck
Present work	(0.704 ± 0.012)	(0.706 ± 0.009)	(0.413 ± 0.006)
Halse (Ref. 4)	(0.66 ± 0.03)	(0.70 ± 0.03)	(0.41 ± 0.01)
Doezema *et al.* (Ref. 10)	(0.704 ± 0.014)	•••	(0.4125 ± 0.004)

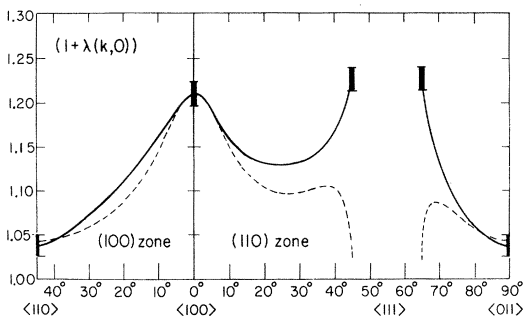

FIG. 2. Angular variation of the factor that describes the renormalization of the one-electron energy bands in copper by the electron-phonon interaction. The full curve and error bars represent the anisotropy of the renormalization factor as determined in the course of the present work; the broken curve is a plot of the angular variation of the square of the deformation potential and has been scaled to fit the renormalization factor in the ⟨100⟩ direction.

basis on which to interpret the electron surface-states resonances observed in other than symmetry directions.

C. Renormalization Factor

In the final column of Table IV, we have tabulated the renormalization factor $[1+\lambda(\vec{k},0)]$ which, by Eq. (11), is equal to the ratio of the band velocity computed from the nonlocal Chodorow potential, to the quasiparticle velocity obtained by inverting the experimental cyclotron-mass data. For reasons discussed above, we believe that the dominant effects of the electron-electron interaction have been folded into the potential; thus, the ratio of velocities is a measure of the renormalization of the one-electron energy bands by the electron-phonon interaction. The renormalization factor is plotted in Fig. 2. It is markedly anisotropic; indeed our calculations provide the first evidence for a systematic anisotropy of the renormalization of the one-electron energy bands in copper by the electron-phonon interaction.

Perhaps the most surprising feature of our results is that the renormalization factor varies significantly over the belly region of the Fermi surface; this is most evident if one compares the renormalization factors appropriate to the belly points in the ⟨100⟩ and ⟨110⟩ directions. We have found that the anisotropy of the renormalization factor may be described qualitatively in terms of a simple model of the electron-phonon interaction based on deformation-potential theory. The matrix element for scattering of an electron from an occupied state $\vec{k}$ to an unoccupied state $\vec{k}'$ by a phonon whose wave vector is $\vec{q}$ and whose polarization is σ is given by Eq. (14), where[34]

$$\mathcal{J}_{\vec{q},\sigma}(\vec{k},\vec{k}') = \int \psi_{\vec{k}}^{*}\,[\delta E_{\vec{k}}(\vec{q}\,\vec{e}_{\vec{q},\sigma})]\,\psi_{\vec{k}'}\,d^3r\,. \qquad (23)$$

The tensor $(\vec{q}\,\vec{e}_{\vec{q},\sigma})$ represents the amplitude of the strain field due to the phonon, and $\delta E_{\vec{k}}(\vec{q}\,\vec{e}_{\vec{q},\sigma})$ is the change in the energy of an electron in state $\vec{k}$ caused by the strain field. For long-wavelength longitudinal phonons, the strain field may be approximated by a pure compression, and the scattering matrix elements are then proportional to the deformation potential, which is defined as the rate of change of the energy of an electron state on the Fermi surface with respect to dilatation, i.e.,

$$E_{\mathrm{def}}(\vec{k}) = [\delta E_{\vec{k}}(\Delta)/\Delta]\,.$$

The deformation potential may be determined from experimental measurements of the pressure dependences of the extremal cross-sectional areas of the Fermi surface. In Table VI, we have compiled the results of experimental studies[2,35] of the pressure dependences of the areas of several extremal orbits on the Fermi surface of copper. We were able to construct a phase-shift model to fit the area changes,[36] and from this model we deduced the pressure dependence of the Fermi wave vector at each point on the Fermi surface. But the band velocity is also known at each point on the Fermi surface. From these two quantities the pressure dependence of the energy of a state of given wave vector may be deduced, and the variation of the deformation potential over the Fermi surface may be computed. Values of the deformation potential at points in the (100) and (110) zones are set out in Table VII.

By combining Eqs. (14), (16), and (23), one finds that the renormalization factor at a point on the Fermi surface may be expressed as an integral involving the square of the deformation potential at that point. In Fig. 2, we have superimposed the angular variation of the square of the deformation

TABLE VI. Pressure derivatives of the extremal cross-sectional areas of certain orbits on the Fermi surface of copper. The orbits are labeled as in Ref. 5. The absolute areas A_0 are estimated from data given by Templeton (Ref. 35) and by O'Sullivan and Schirber (Ref. 2), and are expressed in free-electron units (units of 5.8363 Å^{-2}).

Orbit	A_0	$[10^7\times(\Delta A/A_0)/\Delta P]\mathrm{kg}^{-1}\ \mathrm{cm}^2$ (Ref. 35)	(Ref. 2)	a
B_{100}	0.9810 ±0.0010	•••	4.51±0.2	4.52
B_{111}	0.9504 ±0.0010	4.21±0.04	4.16±0.2	4.19
N_{111}	0.03558±0.00004	19.3 ±0.8	17.6 ±2.0	18.5
D_{110}	0.4112 ±0.0004	•••	3.92±0.2	3.77
R_{100}	0.4027 ±0.0005	•••	4.21±0.3	4.43

[a]Pressure derivatives computed from the phase-shift fit to the experimental data. No attempt was made to optimize the fit in a weighted least-squares sense.

TABLE VII. Anisotropy of the dilatation component of the deformation potential on the Fermi surface of copper. The angle is measured from ⟨100⟩.

(100) zone		(110) zone	
Angle	$E_{def}(\vec{k})$ Ry [a]	Angle	$E_{def}(\vec{k})$ Ry [a]
⟨100⟩	0.4094	⟨100⟩	0.4094
5°	0.3850	5°	0.3871
10°	0.3427	10°	0.3441
15°	0.2987	15°	0.3085
20°	0.2638	20°	0.2867
25°	0.2369	25°	0.2771
30°	0.2169	30°	0.2784
35°	0.2023	35°	0.2852
40°	0.1933	40°	0.2858
⟨110⟩	0.1902	41°	0.2822
		42°	0.2741
		43	0.2587
		44°	0.2298
		45°	0.1517
		neck	0.1325
		65°	0.2004
		66°	0.2395
		67°	0.2557
		68°	0.2625
		70°	0.2629
		75°	0.2386
		80°	0.2127
		85°	0.1966
		⟨110⟩	0.1902

[a] In calculating the deformation potential, we have assumed for the volume compressibility of copper the value quoted by Templeton, namely, $-(1/V)(dV/dP) = 6.907\times10^{-7}$ kg^{-1}cm^2. On the free-electron model the deformation potential would of course be isotropic; its numerical value would be $E_{def}(\vec{k}) = (2E_F^0/3) \approx 0.345$ Ry.

potential upon a plot of the renormalization factor. The square of the deformation potential has been scaled to fit the value of the renormalization factor in the ⟨100⟩ direction. It will be seen that the two functions are in good qualitative agreement with one another except within a few degrees of the necks. Apparently the anisotropy of the matrix element of the electron-phonon interaction determines the anisotropy of the renormalization factor $[1+\lambda(\vec{k},0)]$ on the belly of the Fermi surface of copper; it seems that other influences, such as the anisotropy of the local density of states, may be of lesser importance.

Within a few degrees of the necks the deformation-potential analysis underestimates the magnitude of the renormalization factor. This is perhaps not surprising since the electron states on the necks have p-like symmetry, and they may well couple more strongly to phonons than do the s-like states on the belly. Furthermore, one expects transverse phonons to contribute significantly to electron-phonon processes on strongly aspherical regions of the Fermi surface, such as the necks in copper, and our simple calculations based on the dilatation component of the deformation potential do not apply to such processes. A first-principles calculation taking into account the complexities of the phonon spectrum, the electronic structure, and the electron-phonon interaction would be desirable, both to explain why the deformation-potential analysis works so well on the belly, and to understand in detail the processes that contribute to its failure on the necks.

D. Electron-Phonon Relaxation Time

So far we have been concerned exclusively with the contribution of the electron-phonon interaction to the real part of the proper self-energy. This term corresponds to the emission and absorption of virtual phonons, and leads to a renormalization of the one-electron energy bands. The imaginary part of the proper self-energy corresponds to real processes of phonon emission and absorption; such processes result in the decay of quasiparticle excitations in a manner that can be described approximately by an anisotropic and temperature-dependent relaxation time $\tau(\vec{k})$.

The inverse relaxation time $[1/\tau(\vec{k})]$ for decay of a quasiparticle in state $\vec{k}$ by real electron-phonon processes may be expressed in terms of the matrix elements of the electron-phonon interaction by the integral[37]

$$\frac{\hbar}{\tau(\vec{k})} = \frac{2\Omega}{(2\pi)^2}\sum_\sigma \int \frac{dS_{\vec{k}'}}{\hbar V_{\vec{k}'}} \frac{|M_\sigma(\vec{k},\vec{k}')|^2}{\sinh(\hbar\omega_{\vec{k}-\vec{k}',\sigma}/kT)} \,. \quad (24)$$

By comparing Eqs. (16) and (24) one finds

$$[\hbar/\tau(\vec{k})] = 2\pi kT\lambda(\vec{k},0) \quad \text{if } (kT \gg \hbar\omega_{max}) \,.$$

Thus, in the high-temperature limit, the inverse relaxation time is proportional to $\lambda(\vec{k},0)$, which is the low-temperature limit of the renormalization factor. However, at low temperatures the inverse relaxation time given by Eq. (24) is proportional to T^3, and is no longer related in any simple way to $\lambda(\vec{k},0)$.

We have shown above that the anisotropy of the renormalization factor is apparently dominated by that of the matrix elements of the electron-phonon interaction. In view of the similarity in structure between Eqs. (16) and (24), it seems likely that the anisotropy of $[1/\tau(\vec{k})]$ is also dominated by that of the matrix elements of the electron-phonon interaction. Since at low temperatures the thermally excited phonons that cause quasiparticle scattering are of predominantly long wavelength, one might expect a deformation-potential calculation of the matrix elements to describe with some accuracy the variation of the phonon-induced relaxation time over the Fermi surface. This leads to an estimate

of the anisotropy of the relaxation time

$$\tau(\vec{k}) \propto [1/E_{\rm def}(\vec{k})]^2 , \tag{25}$$

where $E_{\rm def}(\vec{k})$ is taken from Table VII, and suggests as an independent estimate of this quantity

$$\tau(\vec{k}) \propto [1/\lambda(\vec{k}, 0)]^2 , \tag{26}$$

where $\lambda(\vec{k}, 0)$ is taken from Table IV.

In Fig. 3, we have plotted the anisotropy of the relaxation time as deduced from Eqs. (25) and (26). The accuracy of the determination of $\lambda(\vec{k}, 0)$ is such that the relaxation time cannot be estimated very accurately from the renormalization factor. The results suggest that $\tau(\vec{k})$ varies significantly over the belly of the Fermi surface of copper, the relaxation time at ⟨110⟩ being perhaps five times greater than at ⟨100⟩. The average of $[1/\tau(\vec{k})]$ that describes the relaxation time for a quasiparticle in a cyclotron orbit is given by

$$\frac{1}{\tau_0} = \oint_{\rm orb} \frac{[1/\tau(\vec{k})]}{V_\perp(\vec{k})}\, dk \Big/ \oint_{\rm orb} \frac{1}{V_\perp(\vec{k})}\, dk \tag{27}$$

and the relationship between $(1/\tau_0)$ and $[1/\tau(\vec{k})]$ parallels that between λ_0 and $\lambda(\vec{k}, 0)$.

The special features of the electron-phonon interaction on the necks, that caused the deformation-potential calculation to underestimate the extent of the renormalization on this region of the Fermi surface, apply also to real electron-phonon processes. Furthermore, while the integrands in Eqs. (16) and (24) are similar in structure, the exponential denominator in Eq. (24) weights small-angle processes (for which $\hbar\omega_{\vec{k}-\vec{k}'} \ll kT$) much more strongly than does the linear denominator in Eq. (16), and one might expect that the increased local density of states on the necks in copper would play a relatively greater role in enhancing the inverse relaxation time than it does in enhancing the renormalization factor. Hence we have no reason to assume that the inverse relaxation time on the necks is proportional either to the square of the deformation potential, or to the renormalization factor, and a first-principles calculation would probably be needed to investigate the anisotropy of the relaxation time on this region of the Fermi surface.

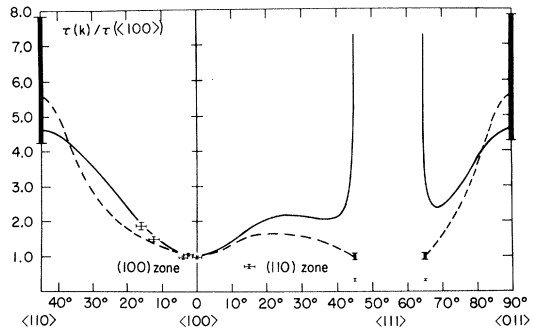

FIG. 3. Estimates of the anisotropy of the $(1/T^3)$-dependent component of the relaxation time for quasiparticle excitations in copper. The full curve is a plot of the relaxation time as computed from the deformation potential, while the broken curve and associated error bars represent the relaxation time as estimated from the renormalization factor. For reasons discussed in the text, we would not expect either of these approximations to describe accurately the variation of the relaxation time close to the necks. The points (added in proof) represent experimental data of Koch and Doezema (Ref. 39).

An experimental investigation of the anisotropy of the temperature-dependent component of the quasiparticle relaxation time in copper has been carried out by Häussler and Welles,[38] who measured the damping of cyclotron resonance curves corresponding to the (100) belly and the neck orbits, and found that $(\tau_B/\tau_N) \approx 10$, with an estimated uncertainty of a factor of 2. Results of an investigation by Koch and Doezema,[39] based on studies of the damping of electron surface-state resonances, show that the relaxation time increases away from the ⟨100⟩ belly point in the (100) zone in a way that is consistent with the results of the deformation-potential calculation. However, their single measurement in the (110) zone suggests that in this zone the relaxation time decreases away from ⟨100⟩, contrary to the prediction of the deformation-potential calculation. The experimental data of Koch and Doezema are superimposed on our theoretical estimates of the anisotropy of the relaxation time in Fig. 3.

Koch and Doezema find also that the ratio between the relaxation times at the ⟨100⟩ belly point and on the necks is

$$(\tau_{\langle 100\rangle}/\tau_{\langle \rm neck\rangle}) \approx (3.0 \pm 0.1). \tag{28}$$

If we may assume that the deformation-potential calculation describes correctly the anisotropy of the relaxation time on the belly, then we can evaluate the relaxation time for the (100) belly orbit by numerical integration of Eq. (27). We find

$$(\tau_B/\tau_{\langle 100\rangle}) \approx 1.95 .$$

This result may be combined with the experimental result of Koch and Doezema [Eq. (28)] to give

$$(\tau_B/\tau_N) \approx 5.85 ,$$

which is consistent with the experimental result of Häussler and Welles. Thus the deformation-potential calculation of the relaxation time for states on the belly of the Fermi surface of copper is generally consistent with current experimental data.

Nevertheless, further experimental work is needed, both to test more critically the predicted anisotropy of the relaxation time on the belly, and to determine its variation on the necks.

CONCLUSIONS

In an earlier paper, the method of phase-shift analysis was applied to interpret experimental data concerning the shape of the Fermi surface of copper, and to construct a one-electron potential that is consistent both with experimental Fermi-surface data and with the energies of several interband optical transitions. In the present paper, we have extended the range of application of the phase-shift method to explore certain of the dynamical properties of quasiparticle excitations in copper.

We began by devising an interpolation scheme for the experimental cyclotron-mass data. A model involving three adjustable phase shifts gave an encouraging, if approximate, fit to the data, and a cubic harmonic expansion of the residuals was rapidly convergent. We found that the masses derived from this interpolation scheme are entirely consistent with the experimental cyclotron masses. The variation of the quasiparticle velocity over the Fermi surface was determined from the interpolation scheme. Our results are in good over-all agreement with Fermi velocities computed by Halse in the course of an analysis of experimental cyclotron-mass data by an independent technique. There is a slight discrepancy between the two estimates of the Fermi velocity in the $\langle 100 \rangle$ direction, but this may reflect only the greater number of cyclotron masses that are taken into account in the present calculations. Our results are in good agreement with the experimental Fermi velocities in the $\langle 100 \rangle$ direction, and on the neck, as determined by Doezema, Koch, and Strom.

Our results show that the renormalization of the one-electron energy bands by the electron-phonon interaction varies significantly over the Fermi surface. We found that for states on the belly the anisotropy of the renormalization factor is in good qualitative agreement with the predictions of a simple deformation-potential calculation, but that for states on the necks the deformation-potential calculation underestimates the extent of the renormalization. This partial success of the deformation-potential calculation encouraged us to apply similar techniques to discuss the anisotropy of that component of the quasiparticle relaxation time which is associated with the electron-phonon interaction. We proposed a model to describe the variation of the electron-phonon relaxation time over the belly, but in view of the complexity of the electron-phonon interaction on the necks, we concluded that a first-principles calculation would probably be needed to extend the model into that region of the Fermi surface. There are at present few experimental data concerning the anisotropy of the electron-phonon relaxation time in copper, but our empirical deformation potential may assist in the interpretation of such data when they become available.

We chose copper as the subject of this investigation largely because the electronic properties of copper have been studied in greater detail, both experimentally and theoretically, than have those of any other metal. In part, this is a consequence of the favorable metallurgical properties of copper, and of the relative simplicity of its Fermi surface. But the electronic properties of copper are of special interest because copper may be regarded as the simplest of the $3d$ transition metals. Its Fermi surface, although derived from s-p-like energy bands, is strongly perturbed by d-like bands that lie just below the Fermi energy. Our success in applying the phase-shift method to investigate the dynamical properties of quasiparticle excitations in copper suggests that this method may prove equally fruitful in investigations of the corresponding properties both of simple metals, for which it is rivaled by pseudopotential techniques, and of transition metals, for which alternative techniques of analysis have yet to be developed.

ACKNOWLEDGMENTS

I wish to thank Professor M. H. Cohen for suggesting the deformation-potential calculation of the renormalization factor, and to thank Professor J. F. Koch and R. E. Doezema for helpful discussions concerning the electron surface-state resonance experiments. I am also indebted to Professor J. F. Koch and R. E. Doezema, and to Dr. M. R. Halse and Dr. D. Shoenberg for communicating to me certain of their results prior to publication. This research was supported in part by the U.S. Army Research Office (Durham), and benefited from the use of facilities provided by the Advanced Research Projects Agency for materials research at the University of Chicago. In carrying out this research I was greatly assisted by the facilities of the Computation Center of the University of Chicago.

---

[1]J.-P. Jan and I. M. Templeton, Phys. Rev. 161, 556 (1967).

[2]W. J. O'Sullivan and J. E. Schirber, Phys. Rev. 170, 667 (1968); 181, 1367 (1969).

[3]A. S. Joseph, A. C. Thorsen, E. Gertner, and L. E E. Valby, Phys. Rev. 148, 569 (1966).

[4]M. R. Halse, thesis, University of Cambridge, 1968 (unpublished); Phil. Trans. Roy. Soc. (London) A265, 507 (1969).

[5]M. J. G. Lee, Phys. Rev. 187, 901 (1969).

[6]J. F. Koch, R. A. Stradling, and A. F. Kip, Phys. Rev. 133, 240 (1964).

[7]D. A. Smith, Proc. Roy. Soc. (London) A296, 476 (1967).

[8]A. F. Kip, D. Langenberg, and T. W. Moore, Phys. Rev. 124, 359 (1961).

[9]D. J. Roaf, Phil. Trans. Roy. Soc. (London) A255, 135 (1962).

[10]R. E. Doezema, J. F. Koch, and U. Strom, Phys. Rev. 182, 717 (1969); and (private communication).

[11]T. W. Nee, J. F. Koch, and R. E. Prange, Phys. Rev. 174, 758 (1968).

[12]G. Dresselhaus, Solid State Commun. 7, 419 (1969).

[13]M. J. G. Lee, Phys. Rev. 178, 953 (1969).

[14]J. C. Slater, Phys. Rev. 51, 846 (1937).

[15]See, for example, Ref. 5.

[16]We set the lattice constant equal to the value quoted by Halse (Ref. 4), $a_0 = (3.6030 \pm 0.0003)$ Å at i °K, and used a 30×30 secular determinant to compute the Fermi-energy parameter, and set of phase shifts, that gave the best agreement with the Fermi-surface data. The best value of the Fermi-energy parameter was found to be $E_F = 0.550\,000$ Ry, and the corresponding values of the phase shifts were $\eta_0 = 0.058\,119$ rad, $\eta_1 = 0.123\,509$ rad, $\eta_2 = -0.115011$ rad, $\eta_3 = 0.001353$ rad. Subsequently we shall refer to these as the phase shifts at the Fermi energy.

[17]M. I. Chodorow, Ph. D. thesis, MIT, 1939 (unpublished); the potential used in the calculations referred to here was obtained by interpolating the data quoted by G. A. Burdick, Phys. Rev. 129, 138 (1963).

[18]U. Gerhardt, Phys. Rev. 172, 651 (1968).

[19]The correction procedure and numerical results are described more fully in Ref. 5.

[20]See, for example, J. M. Ziman, *Principles of the Theory of Solids* (Cambridge U.P., London, England, 1964), p. 153.

[21]Reference 20, p. 156.

[22]Reference 20, p. 250.

[23]We use ϵ to represent energies measured with respect to the Fermi energy; thus $\epsilon(\vec{k}) = [E(\vec{k}) - E_F]$. We use a superscript 0 to denote unrenormalized energies, masses, and velocities; for renormalized quantities the superscript is omitted.

[24]D. Pines, in *Solid State Physics* (Academic, New York, 1955), Vol. 1, p. 407. For a formal discussion of the renormalization of one-electron energy bands by the Coulomb electron-electron interaction, see, for example, V. Ambegaokar, *Many Body Physics* (Gordon and Breach, New York, 1968), p. 320.

[25]A. B. Migdal, Zh. Eksperim. i Teor. Fiz. 34, 1438 (1958) [Soviet Phys. JETP 7, 966 (1958)].

[26]G. M. Éliashberg, Zh. Eksperim. i Teor. Fiz. 38, 966 (1960) [Soviet Phys. JETP 11, 696 (1960)]; V. Ambegaokar and L. Tewordt, Phys. Rev. 134, A805 (1964); W. L. McMillan, *ibid.* 167, 331 (1968).

[27]G. Grimvall, J. Phys. Chem. Solids 29, 1221 (1968); Solid State Commun. 7, 213 (1969).

[28]cf., W. L. McMillan, Phys. Rev. 167, 331 (1968).

[29]J. M. Ziman, *Electrons and Phonons* (Oxford U.P., London, England, 1960), p. 182.

[30]It seems probable that the rosette mass quoted by Koch, Stradling, and Kip ($m_H \approx 1.40 \pm 0.01$) is in error either through false identification of the orbit or as a consequence of mass spread.

[31]The phase shifts computed from the nonlocal Chodorow potential for $E = 0.550046$ Ry differ from the phase shifts at the Fermi energy (Ref. 16) by the following corrections: $\delta\eta_0 = -2.13 \times 10^{-5}$ rad, $\delta\eta_1 = +1.00 \times 10^{-5}$ rad, $\delta\eta_2 = +1.20 \times 10^{-6}$ rad, $\delta\eta_3 = 0$.

[32]For analytic expressions for the cubic harmonics in a form convenient for computation, see, e.g., M. J. G. Lee and L. M. Falicov, Proc. Roy. Soc. (London) A304, 319 (1968).

[33]The phase shifts determined by constructing a surface of constant energy $E = 0.550\,046$ Ry to fit experimental cyclotron-mass data, differ from the phase shifts at the Fermi energy (Ref. 16) by the following corrections: $\delta\eta_0 = -1.26 \times 10^{-5}$ rad, $\delta\eta_1 = 2.40 \times 10^{-5}$ rad, $\delta\eta_2 = -6.10 \times 10^{-7}$ rad, $\delta\eta_3 = 0$.

[34]Reference 29, p. 194.

[35]I. M. Templeton, Proc. Roy. Soc. (London) A292, 413 (1966).

[36]We calculated the phase shifts required to fit the experimental-pressure data extrapolated to a pressure of 100 kg cm^{-2}. We assumed that the Fermi-energy parameter remains equal to 0.550 000 Ry, and calculated the change in the lattice constant ($\delta a_0 = -8.3 \times 10^{-5}$ Å) from the value of the compressibility quoted by Templeton (Ref. 35). The phase shifts were found to differ from the phase shifts at the Fermi energy (Ref. 16) by the following corrections: $\delta\eta_0 = +4.10 \times 10^{-5}$ rad, $\delta\eta_1 = +2.93 \times 10^{-5}$ rad, $\delta\eta_2 = +6.53 \times 10^{-6}$ rad, $\delta\eta_3 = 0$.

[37]This result is most easily obtained from the Golden Rule of perturbation theory; cf. J. M. Ziman, Phys. Rev. 121, 1320 (1961).

[38]P. Häussler and S. J. Welles, Phys. Rev. 152, 675 (1966).

[39]J. F. Koch and R. E. Doezema (private communication); Phys. Rev. Letters 24, 507 (1970). Our references to this work were substantially revised in proof.